

Fatigue Crack Growth Behaviour of 6013 Aluminium Alloy at Different Ageing Conditions in Two Orientations

Aziz Egemen VARLI

TÜBİTAK-SAGE PK 16 Mamak Ankara-TURKEY

e-mail: avarli@sage.tubitak.gov.tr

Rıza GÜRBÜZ

Middle East Technical University, Metallurgical and Materials Engineering Department
Ankara-TURKEY

Received 27.07.2006

Abstract

The effect of different ageing treatments on the fatigue crack growth behaviour of AA6013 aluminium alloy was investigated. C(T) (Compact Tension) specimens prepared in L-T and T-L orientations were aged under 3 different conditions: T651-peak aged (as received), T42-natural aged (solution heat treated at 538 °C for 90 min, water quenched and aged at room temperature for 96 h), and overaged (T42 temper + overageing at 245 °C for 12 h). Electrical conductivity and hardness measurements were performed to verify the heat treatments. Fatigue crack growth tests were performed on the samples with a stress ratio of $R = 0.1$ and a frequency of 4 Hz. In the T-L orientation, the highest fatigue crack growth resistance was achieved for T651 temper. In the L-T orientation, however, T42 + overageing temper exhibited the highest fatigue performance.

Key words: Fatigue, Crack growth rate, Aluminium alloy, Ageing, AA6013.

Introduction

Age hardenable aluminium alloys are important for the aerospace industry because of their light weight and high-yield strengths. Alloy 6013, which is a member of the age hardenable Al-Mg-Si-(Cu) alloy group, has high corrosion resistance and good weldability. Alloy 6013 is considered a replacement for alloy 2014, which has poor weldability (Williams and Starke, 2003). This new weldable aluminium alloy can be used in the form of extruded panels, to replace the riveted assemblies by welded structures (Rendings, 1997).

Damage tolerant design requirements for aeronautical structures have led to an increase in the number of studies on fatigue life prediction methods that use the parameters of fracture mechanics. In these investigations, crack length, a , versus load cycle, N , data are determined and are analysed to yield

a fatigue crack growth rate, da/dN , as a function of the applied stress intensity range, ΔK (Gürbüz and Sarioğlu, 2001).

This study investigated the effect of ageing conditions and orientation on the fatigue crack growth behaviour of 6013 alloy.

Materials and Experimental Procedure

The medium strength 6013 T651 aluminium alloy used in this investigation was in the form of cold rolled plate from the Aluminium Company of America (ALCOA) with the chemical composition Al-0.70Si-0.25Fe-0.90Cu-0.28Mn-0.90Mg-0.03Cr-0.02Zn-0.02Ti (wt%). T651 temper designation refers to a heat treatment of solutionising at 538 °C, ageing at room temperature for 96 h and artificially ageing at 191 °C for 4-5 h. In addition, the material was stress relieved by stretching to

an amount of 1.5%-3% after solution heat treatment or after cooling from an elevated temperature (ASM International, 1999).

In the case of T42 temper, the original alloy was first solution treated and then artificially aged at room temperature for 96 h. The sample in T42 temper was overaged by artificially ageing at 245 °C for 12 h, and this condition is termed TOA in this paper. All heat treatment processes were achieved using an air convection furnace with a temperature uniformity tolerance of ± 3 °C. Electrical conductivity and hardness measurements were performed to verify the heat treatments. The hardness and electrical conductivity profile of the TOA ageing is given in Figure 1. The final hardness and electrical conductivity values for each heat treatment are tabulated in Table 1.

Compact tension C(T) specimens used in fatigue crack growth tests were machined from the plate in T-L and L-T directions in accordance with the nomenclature of ASTM E 399-99 standard. Fatigue crack growth tests were carried out in accordance with ASTM E 647-00 standard. Tests were per-

formed on a closed loop, servo hydraulic universal testing system operated in the load control mode. Constant amplitude sinusoidal loading was applied with a stress ratio, $R = 0.1$. The frequency of loading was 4 Hz for all tests. Instantaneous crack lengths were measured from 2 opposite surfaces with the aid of crack gauges. The data were collected with an analogue to digital converter card, installed on a computer, and data collecting software. The average crack size was used to plot the crack length (a) versus number of cycle (N) curve. A 7-point incremental polynomial technique was employed to determine the fatigue crack growth rate, da/dN .

Fracture surfaces of the specimens were finally examined by scanning electron microscope (SEM) to highlight the fatigue crack propagation mechanisms.

Results and Discussion

The fatigue crack growth rate diagrams (da/dN vs ΔK) for the 3 ageing conditions are given in Figures 2 and 3 for T-L and L-T orientations, respectively.

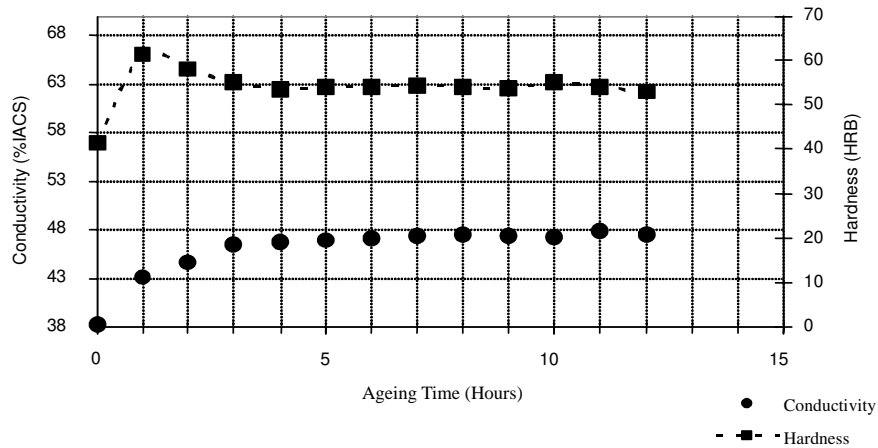


Figure 1. Hardness and conductivity change of TOA aging.

Table 1. Hardness and electrical conductivity after the ageing treatments.

	AA6013 T651	AA6013 T42	AA6013 TOA
Hardness (Rockwell B)	HRB 70-72	HRB 40-42	HRB 52-54
Conductivity (% IACS)	42.5	38.3	47.5

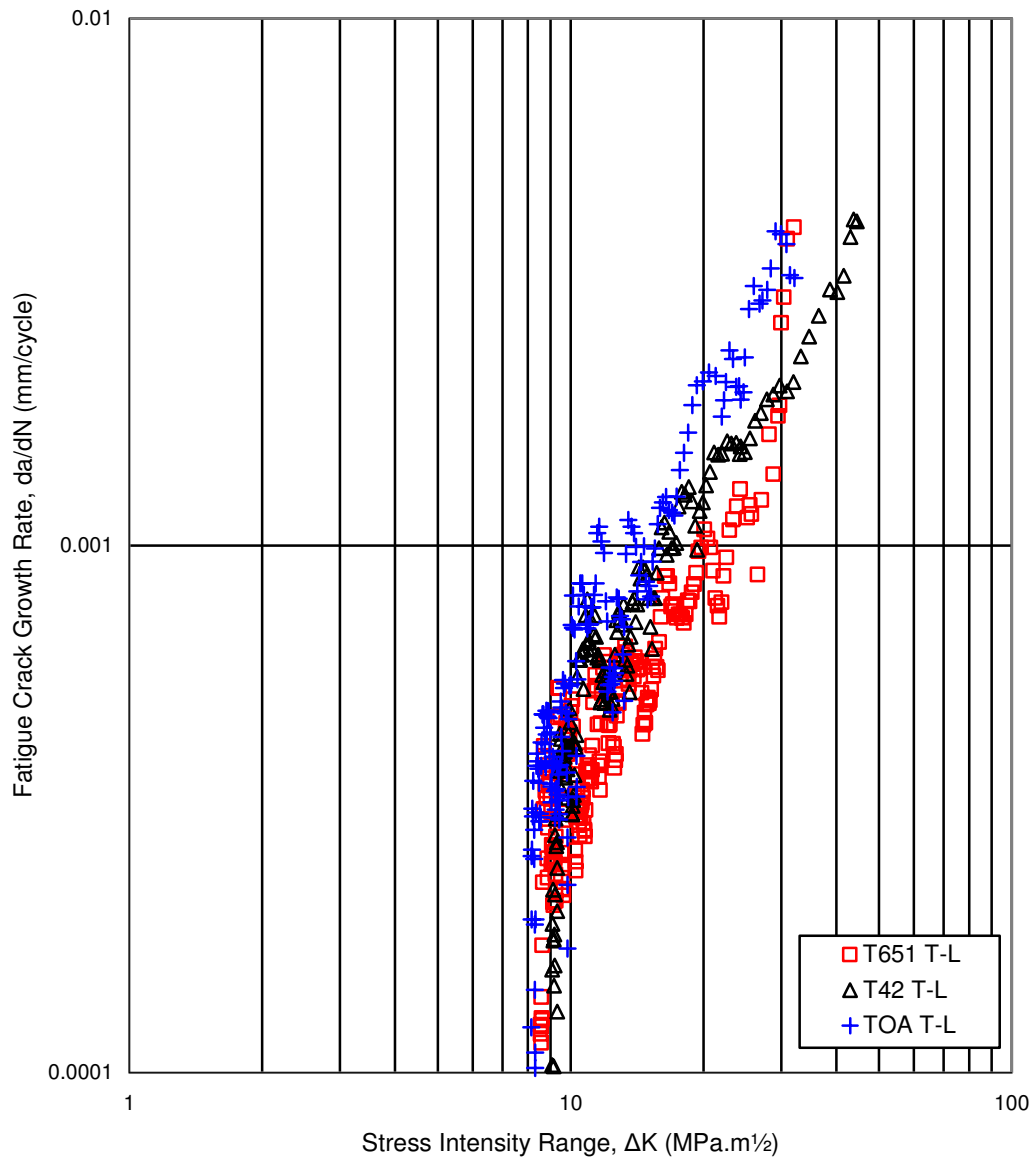


Figure 2. da/dN vs. ΔK plots of three ageing conditions in T-L direction.

As seen in Figure 2, for T-L orientation, the specimen in T651 temper shows the highest resistance to fatigue crack growth rate. Although there is a considerable difference in crack velocities between the 3 ageing conditions at high ΔK levels, the curves become convergent at low ΔK , approaching the threshold values (around $8 \text{ MPa.m}^{1/2}$). The fatigue crack growth rates of specimens at $\Delta K = 20 \text{ MPa.m}^{1/2}$ are given in Table 2. The crack growth rate of T651 is 23% lower than that of T42 and 50% lower than that of TOA condition in the T-L direction. The constants C and m of the Paris-Erdogan relationship $da/dN = C (\Delta K)^m$ (Paris and Erdogan, 1963)

are also tabulated in Table 2.

Figure 3 indicates that the TOA condition exhibits the highest resistance to fatigue crack growth in the L-T orientation. In the contrast, in the T-L orientation, T651 temper has the lowest fatigue crack growth resistance in this direction. Fatigue crack growth resistance was improved by about 38% by TOA ageing, and by 25% by T42 ageing as compared to as-received T651 temper at a ΔK of $20 \text{ MPa.m}^{1/2}$ (Table 2). A similar convergency was observed as the growth rates decrease towards 10^{-4} mm/cycle at a ΔK level of $9 \text{ MPa.m}^{1/2}$.

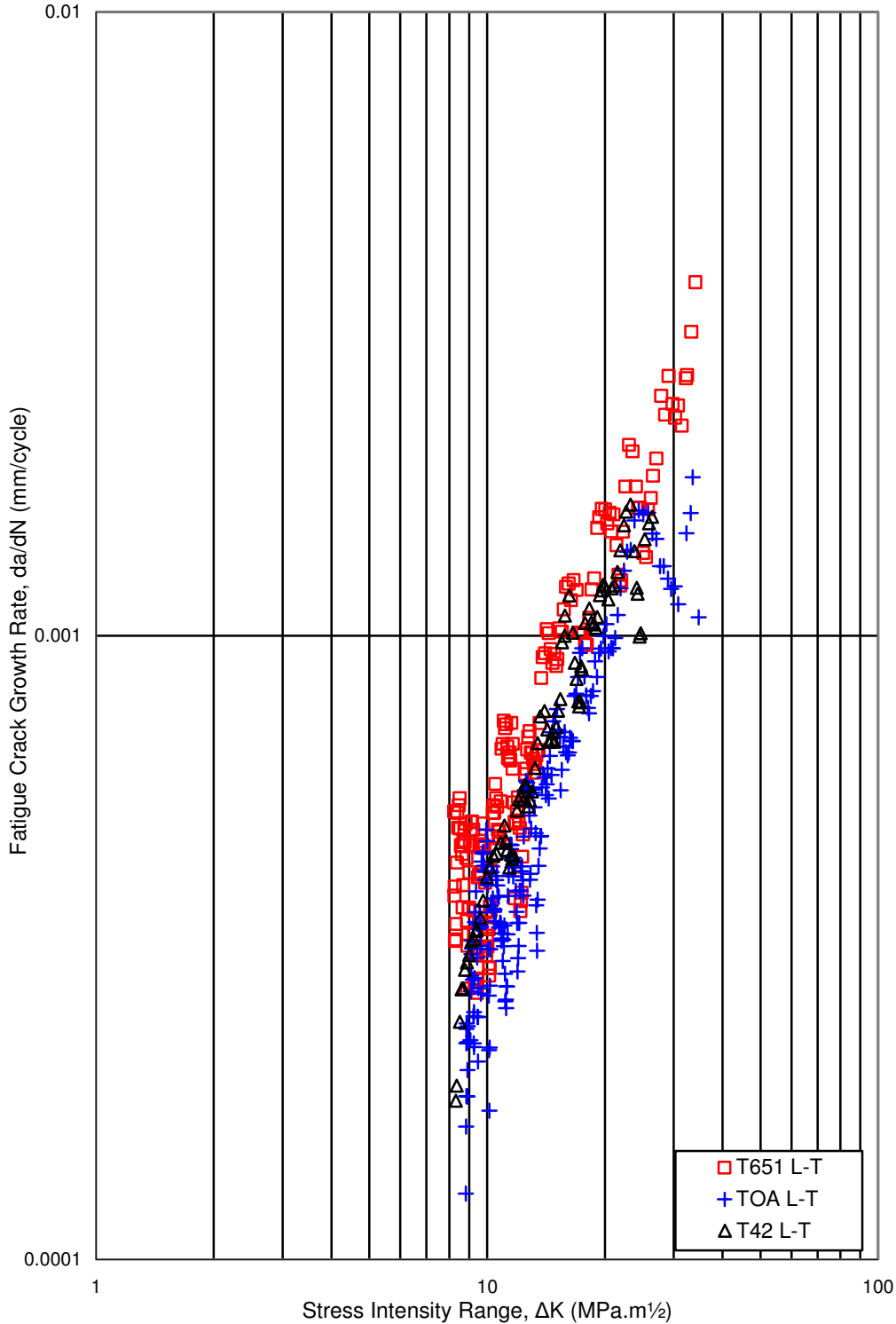


Figure 3. da/dN vs. ΔK plots of 3 ageing conditions in the L-T direction.

Table 2. Crack velocities at $\Delta K = 20 \text{ MPa m}^{1/2}$ and the constants of the Paris-Erdogan equation.

Heat Treatment	Orientation	da/dN at $\Delta K = 20 \text{ MPa m}^{1/2}$ mm/cycle	C	m
T651	T-L	0.0010	7×10^{-6}	1.6589
	L-T	0.0016	1×10^{-5}	1.5159
T42	T-L	0.0013	2×10^{-5}	1.3826
	L-T	0.0012	5×10^{-6}	1.8233
TOA	T-L	0.0020	4×10^{-6}	2.0608
	L-T	0.0010	6×10^{-6}	1.7127

Considering the effect of orientation on the fatigue performance (Table 2), it can be concluded that T-L is better than L-T for T651 condition. There is no considerable difference between the 2 orientations for T42. For TOA, on the other hand, L-T performs better than T-L. Alpay and Gürbüz determined a similar effect of orientation on fatigue crack growth rate of 7050 aluminium alloy for different tempering conditions (Alpay and Gürbüz, 1994).

Fractographic analyses by SEM showed the typical indicators fatigue fracture, like tear ridges, fatigue striations and secondary cracks between striations (Figures 4 and 5). Experimentally determined crack growth rates are well correlated with the growth rates calculated from striation analysis.

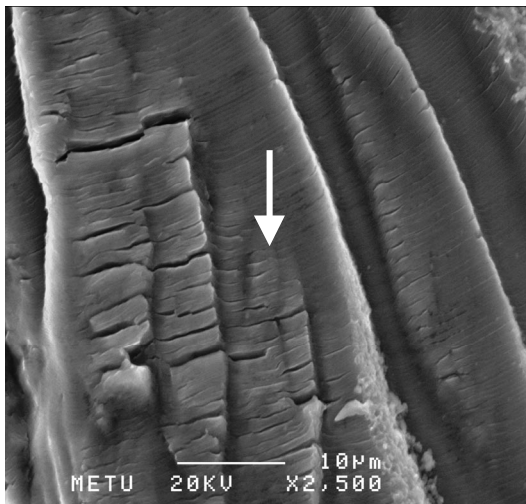


Figure 4. Fractograph of 6013 alloy in T651 T-L condition, showing local micro-cracks with fatigue striations and secondary cracks on them. Arrow indicates the macro-crack growth direction. Crack growth rate is approximately $4.0 \times 10^{-4} \text{ mm/cycle}$.

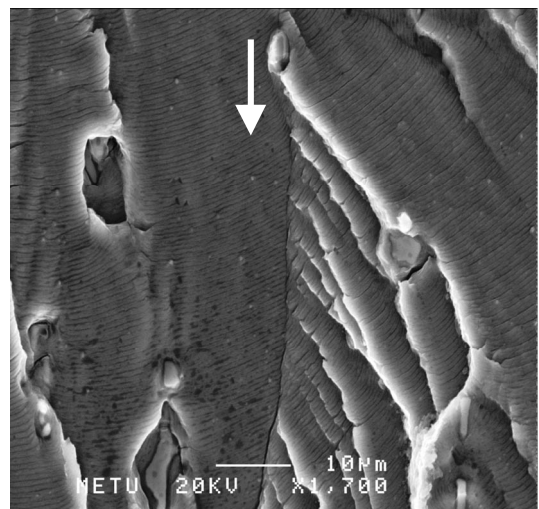


Figure 5. Fractograph of 6013 alloy in TOA L-T condition, showing the coalescence of tear ridges in river pattern mode and local cracks propagating in various directions. Arrow indicates the macro-crack growth direction. Crack growth rate is approximately $5.6 \times 10^{-4} \text{ mm/cycle}$.

Conclusions

The following conclusions can be drawn from the results of this study:

1. In the T-L direction, peak aged T651 condition is more resistant to fatigue crack growth than naturally aged, T42 and overaged, TOA conditions.
2. In the L-T direction, overaged, TOA condition is more resistant to fatigue crack growth than naturally aged, T42 and peak-aged, T651 conditions. Overaging improved fatigue life at all ΔK levels.

Nomenclature

a crack length
N number of cycles

ΔK stress intensity factor range
da/dN fatigue crack growth rate

References

Alpay, S.P. and Gürbüz, R., "Effect of Aging on the Fatigue Crack Growth Kinetics of an Al-Zn-Mg-Cu Alloy in Two directions", *Script. Metall. Mater.*, 30, 423-427, 1994.

ASM, Heat Treaters Guide, Practices and Procedures for Nonferrous Alloys, ASM International, 144-145, 1999.

Gürbüz, R. and Sarioğlu F., "Fatigue crack growth behaviour in aluminium alloy 7475 under different aging conditions", *Materials Science and Technology*, 17, 1539-1543, 2001

Paris, P.C. and Erdogan, F., "A Critical Analysis of Crack Propagation Laws" *Journal of Basic Engineering*, 85, 528-534, 1961.

Rendings, K.H., "Aluminum Structures Used in Aerospace Status and Prospect", *Materials Science Forum*, 217, Part IV, 11-23, 1997.

Williams, J.C. and Starke Jr., E.A., "Progress in Structural Materials for Aerospace Systems", *Acta Materialia*, 51, 5775-5799, 2003.